Transient High Affinity Binding of Tissue Factor Pathway Inhibitor−Factor Xa Complexes to Negatively Charged Phospholipid Membranes†

George M. Willems,*,‡ Marie P. Janssen,‡ Irene Salemink,‡,§ Tze-Chein Wun,|| and Theo Lindhout‡,§

Cardiovascular Research Institute Maastricht and Department of Biochemistry, Maastricht University, Maastricht, The Netherlands, and Monsanto Company, Chesterfield, Missouri

Received September 4, 1997; Revised Manuscript Received December 9, 1997

ABSTRACT: The interaction of tissue factor pathway inhibitor (TFPI), factor Xa, and TFPI−factor Xa complexes with negatively charged phospholipid membranes composed of 25 mol % phosphatidylserine and 75 mol % phosphatidylcholine was studied by ellipsometry. The binding of TFPI *alone* was negligible; factor Xa bound with moderate affinity, with a dissociation constant K_d = 42 nM. Formation of the TFPI−factor Xa complex drastically enhanced the affinity for phospholipid membranes, K_d = 5 nM, compared to that of either protein alone. $TFPI_{1-161}$, a TFPI variant lacking the third Kunitz domain and the positively charged C-terminus did not enhance binding affinity of the factor Xa. Analysis of the kinetics of adsorption and desorption confirmed the equilibrium binding data, although upon longer residence at the lipid membrane the desorption rate of TFPI−factor Xa complexes became slower, indicating an increase in affinity with longer residence of the TFPI−factor Xa complexes at the membrane. In contrast, binding of TFPI−factor Xa complexes in the presence of an excess factor Xa was transient: maximal binding is followed by a slow desorption of the complex. Immunoblot analysis revealed that this desorption was accompanied with cleavage of TFPI by membrane-bound factor Xa. Collectively, our results show that phosphatidylserine containing membranes will accumulate tightly bound TFPI−factor Xa complexes, and that uncomplexed, phospholipid-bound, factor Xa, will cause limited proteolysis of TFPI accompanied by simultaneous release of these complexes from the phospholipid membrane.

The transmembrane protein tissue factor (TF) is currently considered as the main initiator of blood coagulation (*1*−*3*). Upon tissue damage, exposure to the blood of tissue factor in subendothelial cell membranes results in the binding and subsequent activation of circulating factor VII. The TF−factor VIIa complex initiates the coagulation process by activation of factor X and factor IX.

The generation of factor Xa and IXa by TF−factor VIIa is regulated by tissue factor pathway inhibitor (TFPI) in a rather unique pathway: first TFPI assembles with factor Xa in a tight binding complex, thereby inactivating factor Xa. This TFPI−factor Xa complex then associates with high affinity to the TF−factor VIIa complex, forming a quaternary complex that neutralizes the TF−factor VIIa activity (*4*, *5*).

TFPI is a 42 kDa, highly glycosylated, plasma protein that contains three Kunitz type domains, a negatively charged N-terminus, and a positively charged C-terminus (*6*). TFPI circulates in plasma predominantly in complex with lipoproteins at a concentration of 2−3 nM (*7*). Using mutants expressed in mouse fibroblasts it was shown that the first Kunitz domain is essential for the interaction with factor VIIa and that the second domain interacts with the active site of factor Xa (*8*).

The role of the third Kunitz domain and the positively charged C-terminus is, as yet, less clearly defined. On one hand it appears that the C-terminal truncated TFPI variant $TFPI_{1-161}$, which lacks the third Kunitz domain and the C-terminus, retains the inhibitory activity against factor Xa and TF−factor VIIa (*9*, *10*). On the other hand, the anticoagulant effect in plasma of C-terminal truncated variants was much less than that of the native protein (*9*). In a purified model system we showed a more rapid inhibition of TF−factor VIIa by full-length TFPI ($TFPI_{FL}$) than by $TFPI_{1-161}$. It appeared that negatively charged phospholipid membranes accelerated the rate of association of factor Xa with $TFPI_{FL}$ but not with the C-terminal truncated variants (*11*). In contrast, for preformed TFPI−factor Xa complexes, the rate of association with TF−factor VIIa incorporated in phospholipid membranes was unaffected by the third Kunitz domain and the positively charged C-terminus. It should be mentioned, however, that another recent study showed no effect of phospholipids on the TFPI−factor Xa association (*12*). Recently, it was shown that the C-terminus plays a critical role in the binding of TFPI to negatively charged phospholipid membranes (*13*). Taken together, these data suggest a role of the C-terminus in the kinetics of TF−factor VIIa inhibition, presumably mediated by interaction of TFPI or TFPI−factor Xa complexes with negatively charged phospholipid membranes.

The regulatory merits of the unique pathway of TF−factor VIIa inactivation by the TFPI−factor Xa complex are ill

† Supported by Grant 902-26-154 from the Dutch Organization for Scientific Research (NWO).

* Address correspondence to this author at the Cardiovascular Research Institute Maastricht, Maastricht University, P.O. Box 616, 6200 MD Maastricht, The Netherlands. Tel: +31 43 388 1651. Fax: +31 43 367 0916.

‡ Cardiovascular Research Institute Maastricht.

§ Department of Biochemistry, Maastricht University.

|| Monsanto Company.

S0006-2960(97)02194-6 CCC: $15.00
Published on Web 02/18/1998

understood, but it is tempting to speculate that these are related to the enhanced affinity for phospholipid membranes of the TFPI−factor Xa complex compared to TFPI alone. This increased binding of TFPI in complex with factor Xa presumably depends on the much higher affinity of the factor Xa for PSPC membranes compared to the weak interaction of TFPI with PSPC membranes (*13*).

Binding of factor Xa to phospholipid membranes requires acidic phospholipids in the membrane and calcium ions in solution (*14*) and depends upon the presence of γ-carboxylated glutamic acid (Gla) residues in the protein (*15*−*17*). Highest affinity is found for membranes containing phosphatidylserine (PS), the natural acidic phospholipid. It has been suggested that binding of factor Xa involves (coordinated binding via) calcium bridges between protein Gla residues and PS headgroups (*18*). The factor Xa shows a moderate affinity, with reported values of the dissociation constant between 50 and 500 nM for membranes containing 20−30 mol % PS (*18*−*21*).

To unravel the role of membrane association of TFPI and TFPI−factor Xa complexes in the inactivation of TF−factor VIIa complexes, detailed information regarding the equilibrium binding and the residence time of the relevant proteins at the membrane is required. Unfortunately, at present only qualitative data are available on the interaction of TFPI and TFPI−factor Xa complexes with phospholipid membranes (*13*). Here, we report a study of the interaction of TFPI and TFPI−factor Xa complexes with phospholipid membranes using ellipsometry (*22*, *23*) for the quantitative determination of protein binding to planar membranes. Equilibrium binding isotherms were measured and kinetics of adsorption and desorption were analyzed in an attempt to characterize the membrane binding.

MATERIALS AND METHODS

Materials. Bovine serum albumin (BSA, essentially fatty acid free) was from Sigma (St. Louis, MO). 1,2-Dioleoyl-*sn*-glycero(3)phosphocholine (DOPC) and 1,2-dioleoyl-*sn*-glycero(3)phosphoserine (DOPS) were purchased from Avanti Polar Lipids (Alabaster, AL). Enhanced chemiluminescence (ECL) Western blotting detection reagents and Hyperfilm-ECL were provided by Amersham Life Science (Buckinghamshire, England). Nitrocellulose transfer membrane (0.2 μm) was obtained from Protran (Dassel, Germany). Other chemicals used were of analytical grade. Silicon slides were from Aurel GmbH (Landsberg, Germany).

Proteins. Purified human factor X (*24*) was activated and isolated as described earlier (*25*). Factor Xa was quantified as described before (*26*). Recombinant full-length human tissue factor pathway inhibitor ($TFPI_{FL}$) was produced in *Escherichia coli* as described before (*27*) and was kindly supplied by Searle/Chiron (Chesterfield, MO/Emeryville, CA). This recombinant TFPI preparation, being not glycosylated, has a molecular weight of 32 kDa but is very similar to the native glycosylated protein expressed in mammalian cells with respect to factor Xa inhibitory activity and anticoagulant activity (*27*, *28*). The C-terminal truncated variant of TFPI lacking the C-terminus and the third Kunitz domain, $TFPI_{1-161}$, expressed in *Saccharomyces cerevisiae* and purified as described (*29*) was a kind gift of Dr. O. Nordfang (Novo Nordisk, Gentofte, Denmark). The molar concentrations of TFPI preparations were determined by titration with known amounts of factor Xa (*30*). Polyclonal goat anti-human $TFPI_{1-161}$ antibodies (*31*) were a kind gift of Dr. O. Nordfang (Novo Nordisk, Gentofte, Denmark). Swine anti-goat IgG, labeled with horseradish peroxidase, was purchased from Caltag Laboratories (San Fransisco, CA).

Phospholipid Bilayers. Phospholipid concentrations were determined by phosphorus analysis (*32*). Planar bilayers were deposited on silicon slides as described previously (*33*). Briefly, small unilamellar vesicles were prepared by sonication of a mixture of 25 mol % DOPS and 75 mol % DOPC (PSPC). The silicon slides were thoroughly cleaned, treated with chromic sulfuric acid, and rinsed extensively with water before use. A planar bilayer was deposited on the slide by immersion for 5 min in a stirred suspension of small unilamellar phospholipid vesicles (30 μM) in Tris buffer (50 mM Tris, 175 mM NaCl, 3 mM $CaCl_2$, pH 7.5).

Ellipsometric Determination of Protein Adsorption to Lipid Bilayers. Measurement of protein adsorption to planar bilayers by ellipsometry has been described extensively (*21*−*23*). Briefly, the technique is based on the change in reflection coefficients of reflecting surfaces, e.g. silicon surfaces, as a consequence of the adsorption of thin (0.1−10 nm) lipid or protein films. Such changes result in an alteration of the polarization state of reflected light that can be accurately measured using an ellipsometer. The instrument and data analysis were as described (*22*, *23*). In this study we used silicon slides and an angle of incidence of 68°, and under these conditions the mass, $\Gamma(t)$ (μg cm^{-2}), of adsorbed protein (or phospholipid) is proportional to the change, $\delta P(t)$, in the polarizer reading (degrees) caused by the adsorption: $\Gamma(t) = 0.085\delta P(t)$. Protein adsorption experiments were performed in a trapezoidal cuvette at ambient temperature (20−22 °C) in Tris buffer (50 mM Tris, 175 mM NaCl, 3 mM $CaCl_2$, pH 7.5). Protein adsorption was initiated by addition of a small aliquot (<250 μL) of a protein solution to the cuvette (4 mL). To avoid nonspecific depletion of protein, the cuvette walls were blocked by a preincubation with Tris buffer containing 10 mg mL^{-1} BSA during 15 min. Desorption of protein was started by depletion of the protein from the solution in the cuvette by flushing the cuvette (4 mL) with Tris buffer (30−60 mL). Accumulation of protein released from the planar lipid membrane was prevented by refreshment of the cuvette solution at a flow rate of 1 mL min^{-1}.

Analysis of Equilibrium Binding. Measurements of equilibrium binding as a function of the solution concentration of protein were analyzed by using the Langmuir model for independent binding sites:

$$\Gamma_{eq} = \Gamma_{max} C/(K_d + C) \quad (1)$$

which relates the amount of protein (Γ_{eq}) bound on the membrane to the protein concentration in solution (C), the dissociation constant (K_d), and the maximal protein adsorption (Γ_{max}). The binding parameters K_d and Γ_{max} are estimated by a least-squares fit of this model to experimental data.

Analysis of the Kinetics of Protein Adsorption and Desorption. The adsorption and desorption kinetics of protein to the planar membrane are determined not solely by intrinsic adsorption and desorption rates but also by the rate of mass

transfer of protein from bulk solution to the adsorbing macroscopic surface. The mass transfer from bulk solution to the surface, effected by convection and diffusion, depends on the flow configuration and the diffusion coefficient of the protein. This mass transport, J (μg cm^{-2} s^{-1}), is equal to the mass transfer coefficient Δ (cm s^{-1}), which depends on the experimental setup (flow conditions) and the diffusion constant of the protein, times the difference between the concentration in bulk solution, C_b (μg mL^{-1}), and the concentration, C_o (μg mL^{-1}), near the adsorbing surface:

$$J = \Delta(C_b - C_o) \quad (2)$$

Thus the protein in the fluid immediately adjacent to the adsorbing surface is depleted, i.e., $C_o < C_b$. In previous studies we have shown that in this situation equilibrium exists between bound protein Γ (μg cm^{-2}) and the local concentration C_o at the phospholipid membrane−buffer interface near the PSPC membrane, i.e., $C_o = K_d\Gamma/(\Gamma_{max} - \Gamma)$ according to eq 1. Insertion of this relation between C_o and Γ in eq 2 results in the following differential equation for the description of the adsorption and desorption kinetics (*34, 35*):

$$(d/dt)\Gamma = \Delta(C_b - C_o) = \Delta(C_b - K_d\Gamma/(\Gamma_{max} - \Gamma)) \quad (3)$$

This equation predicts that initially, at a low surface coverage, the adsorption rate is equal to the transport limit, ΔC_b. With increasing surface coverage, the adsorption rate will decrease proportionally to the dissociation constant, K_d, times $\Gamma/(\Gamma_{max} - \Gamma)$. Equation 3 also allows analysis of desorption kinetics as measured after depletion of protein from the buffer solution. If the maximal binding capacity, Γ_{max}, is identified from equilibrium binding, measurement of the kinetics of adsorption or the kinetics of desorption allows thus determination of the dissociation constant. To this end, the kinetics of protein adsorption and desorption were analyzed by a least-squares fit of the numerical solution of eq 3 to the data.

Proteolysis of TFPI and Immunoblot Analysis. $TFPI_{FL}$ (6 nM) was incubated with factor Xa (18 nM) in the presence and absence of PSPC vesicles (10 μM) in Tris buffer. The reaction was stopped by adding the samples to the sample buffer for SDS−PAGE (final concentrations: 0.075 M Tris-HCl, pH 6.7 containing 0.7% SDS, 1.25% β-mercaptoethanol, 10% glycerol, and 0.25% bromophenol blue). Then samples were incubated for 15 min at 100 °C. After SDS−PAGE (12% separating gel), the samples were electroblotted onto nitrocellulose (0.2 μm pore size) and blocked with 5% nonfat dry milk in PBS (10 mM KH_2PO_4, 150 mM NaCl, pH 7.2). After incubation with a goat polyclonal antibody directed against human $TFPI_{1-161}$ in a PBS-Tween buffer (10 mM KH_2PO_4, 150 mM NaCl, pH 7.2, 0.3% Tween-20) containing 1 mg mL^{-1} BSA, a secondary antibody conjugated with peroxidase was utilized for antigen detection on the nitrocellulose by using the chemiluminescence system of Amersham Life Science (Buckinghamshire, England).

RESULTS

In an exploratory series of experiments, we compared the binding of factor Xa, TFPI, and TFPI−factor Xa complexes to phospholipid membranes composed of 25 mol % DOPS and 75 mol % DOPC. Protein adsorption to phospholipid membranes was measured by ellipsometry.

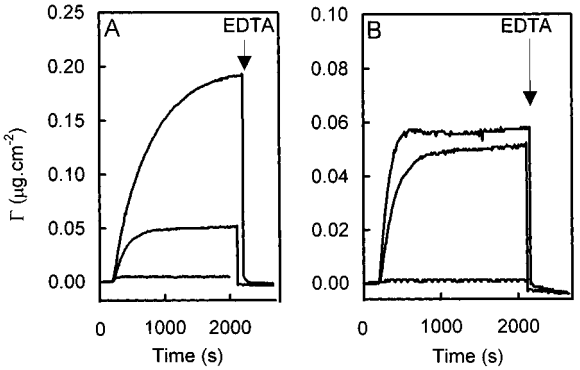

FIGURE 1: Adsorption of TFPI, factor Xa, and TFPI−factor Xa complexes to PSPC bilayers containing 25 mol % PS. At $t = 200$ s, protein was added to the cuvette and adsorption to the phospholipid membrane was measured by ellipsometry. (A) Bottom curve, $TFPI_{FL}$ (20 nM); middle curve, factor Xa (6 nM); top curve, preformed $TFPI_{FL}$−factor Xa complexes (6 nM factor Xa/20 nM $TFPI_{FL}$). At $t \sim 2100$ s, EDTA (5 mM) was added to the cuvette in order to deplete the free calcium ions (3 nM) from the solution. (B) Similar experiments were performed with $TFPI_{1-161}$. Bottom curve, $TFPI_{1-161}$ (20 nM); middle curve, factor Xa (6 nM); top curve, preformed $TFPI_{1-161}$−factor Xa complexes (6 nM factor Xa/20 nM $TFPI_{1-161}$). At $t \sim 2100$ s, EDTA (6 mM) was added. Experiments were performed at ambient temperature (20−22 °C) in Tris buffer (50 mM Tris, 175 mM NaCl, 3 mM $CaCl_2$, pH 7.5).

Because formation of TFPI−factor Xa complexes under the conditions used requires several minutes (*30, 11*), preformed TFPI−factor Xa complexes, prepared by incubation of factor Xa (240 nM) with TFPI (800 nM) for 15 min, were used. Using the rate constants for TFPI−factor Xa association (*30, 11*) it was calculated that 99% of factor Xa is in complex with TFPI. This incubation mixture is 40-fold diluted in the ellipsometer cuvette (100 μL added to 4 mL) resulting in a final concentration of 6 nM TFPI−factor Xa complex (and 14 nM free TFPI). The half-time of release of factor Xa from the TFPI−factor Xa complex is 30−40 min and ultimately, after attainment of the new equilibrium in the cuvette, more than 98% and 95% of factor Xa remains in complex with $TFPI_{FL}$ and $TFPI_{1-161}$, respectively.

Figure 1A shows that the addition of factor Xa (6 nM) to the ellipsometer cuvette results in an equilibrium adsorption amounting to $\Gamma = 0.051$ μg cm^{-2}, whereas $TFPI_{FL}$ (20 nM) alone results in a small adsorption of about $\Gamma = 0.004$ μg cm^{-2}. Despite the negligibly small binding to PSPC of $TFPI_{FL}$ itself, $TFPI_{FL}$ in complex with the phospholipid binding protein factor Xa causes a significant enhancement of binding affinity, resulting in a 4-fold higher adsorption ($\Gamma = 0.19$ μg cm^{-2}). Figure 1A also shows that binding of factor Xa and $TFPI_{FL}$−factor Xa complexes requires Ca^{2+} ions in the buffer. That is, depletion of free Ca^{2+} ions from the buffer by addition of EDTA causes immediate desorption of factor Xa and $TFPI_{FL}$−factor Xa complexes from the phospholipid membrane. Figure 1B shows that the C-terminal truncated TFPI variant $TFPI_{1-161}$ in complex with factor Xa completely lacks the facility to enhance the binding affinity of factor Xa.

Equilibrium Binding Isotherms. Figure 2A shows the concentration dependent binding of factor Xa. It is apparent that the adsorption is rapid and that within 5−10 min a stable plateau is reached. Adsorption of $TFPI_{FL}$−factor Xa com-

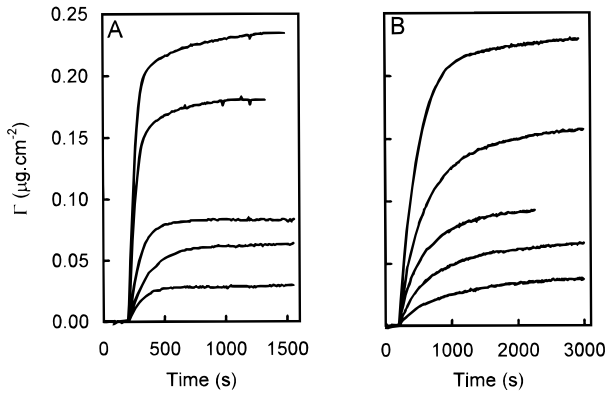

FIGURE 2: Concentration dependent adsorption of factor Xa and TFPI−factor Xa complexes. Protein adsorption was initiated by addition of protein to the buffer at $t = 200$ s, and binding was measured by ellipsometry until a steady state adsorption was attained. (A) adsorption of factor Xa, from bottom to top curve: 4, 8, 12, 25, 50 nM. (B) Adsorption of preformed $TFPI_{FL}$−factor Xa complexes: 1, 2, 3, 6, 12 nM. Preformed $TFPI_{FL}$−factor Xa complexes were prepared by incubation factor Xa (40, 80, 160, 320, and 480 nM) and 800 nM $TFPI_{FL}$ for 15 min. Addition of 100 μL of preincubated mixture to the 4 mL cuvette results in the indicated final concentrations. Further experimental conditions are as in Figure 1, and *y* axis scales are identical in both A and B.

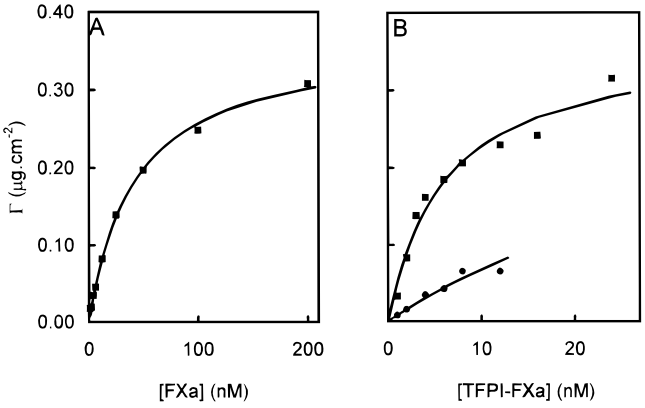

FIGURE 3: Equilibrium isotherms of factor Xa and TFPI−factor Xa binding to PSPC membranes. Plot of measured equilibrium binding as function solution phase concentration. Indicated are mean values of at least two independent measurements. Preformed complexes for concentrations below 14 nM were prepared as described for Figure 2. Higher concentrations of complexes were prepared by incubation of factor Xa with an excess (1.5×) TFPI and were 20-fold diluted upon addition to the cuvette. Panel A, factor Xa binding; panel B, binding of $TFPI_{FL}$−factor Xa complexes (■) and $TFPI_{1-161}$−factor Xa complexes (●). Solid lines indicate the least-squares fit of the Langmuir model (eq 1) to these data. The estimated binding parameters are listed in Table 1, and *y* axis scales are identical in both A and B.

plexes (Figure 2B) requires considerably more time (40−60 min) to approach equilibrium. We further note that the concentrations used in the experiments shown in Figure 2B are 4-fold lower than the concentrations used in Figure 2A. Similar experiments were also performed for $TFPI_{1-161}$−factor Xa complexes. The steady state adsorptions of factor Xa, $TFPI_{FL}$−factor Xa, and $TFPI_{1-161}$−factor Xa, measured in experiments as shown in Figure 2, are replotted in Figure 3 to obtain the binding isotherms of these proteins. An adequate fit of the Langmuir model for independent binding sites (solid line) to these data is apparent. It appears from Figure 3 that the concentrations of the complexes with truncated $TFPI_{1-161}$ used in these binding experiments are

Table 1: Binding Parameters of Factor Xa and TFPI−Factor Xa Complexes Estimated from Equilibrium Binding Experiments[a]

protein	K_d (nM)	Γ_{max} (μg cm^{-2})
factor Xa	42 ± 2.9	0.36 ± 0.01
$TFPI_{FL}$−factor Xa	5.4 ± 0.9	0.36 ± 0.03
$TFPI_{1-161}$−factor Xa	46 ± 3.7	0.36[b]

[a] Equilibrium binding isotherms, as presented in Figure 3, were analyzed using the Langmuir model for independent binding sites (eq 1). Presented are the least-squares fit estimates (±SEM) of the dissociation constant K_d and of the maximal binding Γ_{max}. [b] Fitted with a fixed value $\Gamma_{max} = 0.36$ as obtained for $TFPI_{FL}$−factor Xa complexes.

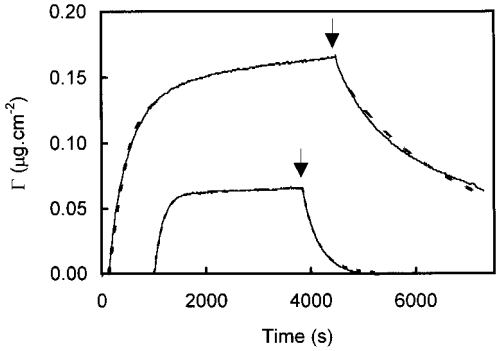

FIGURE 4: Adsorption and desorption kinetics of factor Xa and of $TFPI_{FL}$−factor Xa complexes. Protein adsorption was initiated by addition of $TFPI_{FL}$−factor Xa complex (6 nM at 200 s; upper curve) or factor Xa (8 nM at 1000 s; lower curve) to the cuvette. After protein adsorption reached a steady state, desorption was initiated by depletion of protein from the solution in the cuvette by flushing the (4 mL) cuvette with 30 mL Tris buffer (50 mM Tris, 175 mM NaCl, 3 mM $CaCl_2$, pH 7.5) as indicated in the figure by the arrows. To avoid accumulation of desorbed protein in the buffer, the cuvette solution was refreshed at a rate of 1 mL min^{-1}. The solid lines indicate the measured mass of protein associated to the phospholipid membrane; the dotted lines indicate the best fit of eq 3 to the data. Further experimental conditions are as in Figure 1.

insufficient to saturate the binding, precluding the estimation of Γ_{max} from these data. Therefore the dissociation constant, K_d, was estimated using the value of Γ_{max} found for $TFPI_{FL}$−factor Xa complexes. Table 1 lists the estimated values of the maximal binding, Γ_{max}, and the dissociation constant, K_d. These results show that $TFPI_{FL}$−factor Xa has a 7-fold higher affinity for PSPC membranes than free factor Xa. Interestingly, C-terminal truncated $TFPI_{1-161}$ hardly influences the affinity of factor Xa for the PSPC membrane.

Kinetics of Adsorption and Desorption. Ellipsometric measurements allow determination of protein binding at time intervals of about 10 s, which is sufficiently frequent to define the kinetics of adsorption and desorption of factor Xa and $TFPI_{FL}$−factor Xa complexes as is illustrated in Figure 4. Depletion of protein from the solution initiates desorption of protein associated with the phospholipid membrane. Protein adsorption, both for factor Xa and $TFPI_{FL}$−factor Xa complexes, apparently is reversible, which is in agreement with the Langmuir model presented in the Materials and Methods (eq 3). We used this model to analyze the adsorption and desorption kinetics. In the least-squares fits of eq 3 to the measured protein binding vs time the value of K_d was adjusted, whereas fixed values for maximal binding Γ_{max} as presented in Table 1 (obtained from equilibrium binding experiments) were used. Satisfactory agreement between model and experimental data is shown in Figure 4 for the adsorption and desorption kinetics of

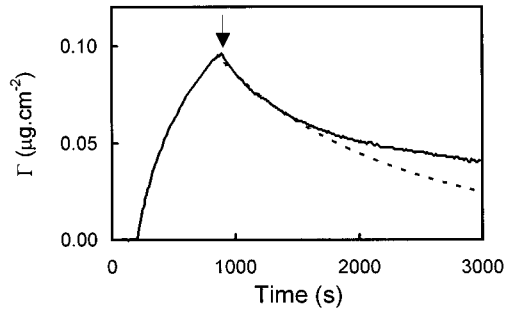

FIGURE 5: Desorption kinetics of $TFPI_{FL}$−factor Xa complexes. Protein adsorption was initiated by addition of $TFPI_{FL}$−factor Xa complex (4 nM at 200 s) to the cuvette. Desorption of protein was initiated by depletion of protein from the solution in the cuvette by flushing the (4 mL) cuvette with 30 mL of Tris buffer, $t = 870$ s (arrow). The solid lines indicate the measured mass of protein associated to the phospholipid membrane; the dotted lines indicate the best fit of eq 3 to the initial 10 min of the data. Further experimental conditions are as in Figure 4.

factor Xa. Also a good agreement was found between fit and data for the adsorption of $TFPI_{FL}$−factor Xa complexes, when the fit was restricted to the initial 10−15 min of the adsorption. For the desorption data of $TFPI_{FL}$−factor Xa complexes the fit in Figure 4 exhibits small but systematic deviations between measurements and model, that suggest a gradual increase in affinity with passage of time. This suspicion was reinforced by the estimation of the K_d value from desorption kinetics of these experiments, in which the desorption was initiated more than 60 min after the start of the adsorption: desorption kinetics indicated an about 6-fold lower value of the K_d than estimated from equilibrium binding (Table 1). Therefore we also studied the kinetics of desorptions that were initiated within 15 min after the start of the adsorption, as shown in Figure 5. When we attempted to fit the entire course of the desorption we again found systematic deviations between fit and data. Restriction of the fit to the initial phase (10 min) of the desorption resulted in a good agreement between fit and data in this 10 min interval, but Figure 5 also shows that beyond this interval deviations arise, indicating that desorption progresses much slower than predicted by the model fit. This fit to experiments as shown in Figure 5 showed 3-fold higher desorption rates, and a correspondingly higher value of $K_d = 2.9 \pm 0.2$ nM (mean value ±SEM, $n = 6$), than experiments in which the desorption was initiated after a residence at the membrane of more than 60 min, confirming a gradual increase of the affinity of $TFPI_{FL}$−factor Xa complexes. Therefore, we limited our analysis of desorption kinetics of $TFPI_{FL}$−factor Xa complexes to the initial 10 min of these experiments in which the desorption was initiated within 15 min after the start of the adsorption. The dissociation constants, estimated from adsorption and desorption kinetics, are presented in Table 2. Both for factor Xa and for factor Xa complexes with C-terminal truncated $TFPI_{1-161}$ a reasonable agreement is found between dissociation constants obtained from kinetics and equilibrium binding. For $TFPI_{FL}$−factor Xa complexes the K_d estimated from desorption kinetics is 50% lower and the K_d estimated from adsorption kinetics is marginally higher than the K_d obtained from equilibrium binding.

PSPC Dependent Factor Xa Mediated Proteolysis of $TFPI_{FL}$. The experiments with TFPI−factor Xa complexes described so far were performed in the presence of an excess TFPI, such that essentially all factor Xa is in complex with TFPI. The residual TFPI remaining uncomplexed does not complicate the experiments as the contribution of this free TFPI to the protein binding is negligible. In contrast, in mixtures with an excess factor Xa, both factor Xa and factor Xa−TFPI complexes contribute to the protein binding measured by ellipsometry. To investigate the effect of an excess factor Xa on the protein binding, we performed experiments as shown in Figure 6. Factor Xa (6 nM) was adsorbed until a steady state level was reached. Next, various concentrations (3, 6, and 20 nM) of $TFPI_{FL}$ were added and the additional binding of $TFPI_{FL}$−factor Xa complexes was monitored by ellipsometry. The adsorption of factor Xa alone reached a stable level of 0.05−0.06 μg cm^{-2} within 10 min. It is seen in Figure 6 that addition of an excess of $TFPI_{FL}$ (20 nM) over factor Xa (6 nM) causes an increase of membrane-bound protein from 0.05 to about 0.17 μg cm^{-2}. Addition of 6 nM $TFPI_{FL}$ instead of 20 nM results in a comparable increase in protein adsorption. As expected, addition of 3 nM $TFPI_{FL}$ resulted in a significantly lower protein adsorption. However, adsorption of the $TFPI_{FL}$−factor Xa complex appeared to be transient. That is, a slow

Table 2: Binding Parameters of Factor Xa and TFPI−Factor Xa Complexes Estimated from Adsorption and Desorption Kinetics

	K_d (nM)	
protein	adsorption kinetics	desorption kinetics
factor Xa	37.0 ± 4.3	28.1 ± 3.2
$TFPI_{FL}$−factor Xa	8.2 ± 0.8	2.9 ± 0.2
$TFPI_{1-161}$−factor Xa	51.4 ± 4.7	28.7 ± 5.4

[a] Protein binding vs time data, as presented in Figures 4 and 5, were analyzed using the Langmuir model for adsorption and desorption kinetics, see eq 3. Values of maximal binding capacity, Γ_{max}, were taken from Table 1. Analysis of desorption kinetics of $TFPI_{FL}$−factor Xa complexes was restricted to the initial kinetics (10 min) of experiments, see Figure 5 and text, in which desorption was initiated within 15 min after the start of the adsorption. Presented are the mean values (± SEM) of the least-squares fit estimates of the dissociation constant K_d, as obtained from adsorption and desorption kinetics of at least 5 experiments.

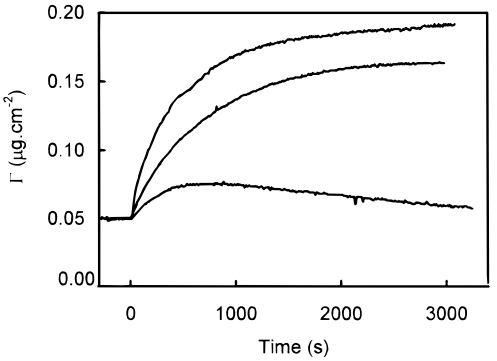

FIGURE 6: Transient adsorption of $TFPI_{FL}$−factor Xa complexes. Factor Xa (6 nM) was added to the cuvette, and the factor Xa adsorption was allowed to reach a steady state ($\Gamma = 0.05$ μg cm^{-2}). $TFPI_{FL}$ was then added to the cuvette ($t = 0$), and the protein adsorption was followed by ellipsometry. For clarity we omitted the factor Xa adsorption and only indicated the extra adsorption on top of the factor Xa adsorption, caused by addition of $TFPI_{FL}$. This extra adsorption is plotted as function of the time after addition of $TFPI_{FL}$ ($t = 0$). Bottom curve, 3 nM $TFPI_{FL}$; middle curve, 6 nM $TFPI_{FL}$; top curve, 20 nM $TFPI_{FL}$. Experimental conditions as in Figure 1.

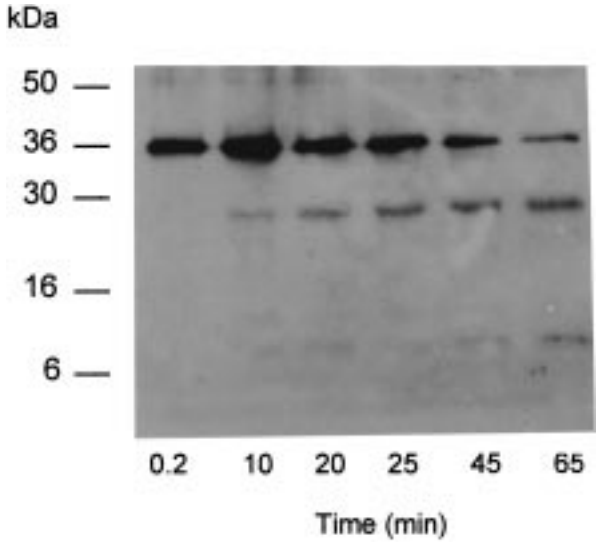

FIGURE 7: Immunoblot analysis of $TFPI_{FL}$ incubated with factor Xa and a PSPC planar bilayer. Reduced samples from the experiment shown by the lower curve of Figure 6, taken at the indicated times after addition of TFPI to the cuvette, were subjected to SDS−PAGE and Western blot analysis using an anti-human $TFPI_{1-161}$ polyclonal antibody as described in the Materials and Methods.

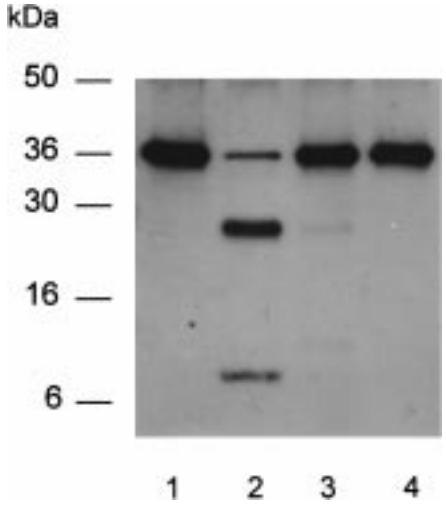

FIGURE 8: Immunoblot analysis of $TFPI_{FL}$ incubated with factor Xa and PSPC vesicles. $TFPI_{FL}$ (6 nM) was incubated for 60 min with 10 μM PSPC vesicles (lanes 2 and 4) or without PSPC (lane 3) either in the presence of factor Xa (18 nM; lane 2 and 3) or in the absence of factor Xa (lane 4). A control sample of $TFPI_{FL}$ is shown in lane 1. Reduced samples were subjected to immunoblot analysis as described (Figure 7 and the Materials and Methods).

desorption of protein is observed after attainment of the maximal adsorption of 0.075 μg cm^{-2}. Since this phenomenon was only observed in the presence of factor Xa in excess over $TFPI_{FL}$, the notion is raised that free factor Xa is likely to alter the phospholipid-binding properties of the $TFPI_{FL}$−factor Xa complex.

To find support for this notion, timed samples, taken from the ellipsometer cuvette that contained 3 nM $TFPI_{FL}$ and 6 nM factor Xa were analyzed by SDS−PAGE and Western blotting using antibodies against $TFPI_{1-161}$. Figure 7 shows the results of this experiment. The 36 kDa band corresponding to $TFPI_{FL}$ slowly disappears, and a 26 kDa and a 8 kDa band appear. No cleavage of $TFPI_{FL}$ was observed if $TFPI_{FL}$ was in excess (20 nM) over factor Xa (6 nM). Experiments in which $TFPI_{FL}$ (6 nM) was incubated with PSPC vesicles (10 μM) and factor Xa (18 nM) at 37 °C showed that after 60 min nearly all $TFPI_{FL}$ was converted into the 26 kDa fragment and the 8 kDa fragment (Figure 8). Figure 8 also demonstrates that cleavage of $TFPI_{FL}$ requires both factor Xa and PSPC membranes. Collectively, these data strongly suggest that desorption of the $TFPI_{FL}$−factor Xa complex from PSPC membranes in Figure 6, is caused by a phospholipid-bound factor Xa mediated proteolysis of $TFPI_{FL}$.

DISCUSSION

Our experiments clearly demonstrate that full-length $TFPI_{FL}$−factor Xa complexes bind with high affinity to PSPC membranes, whereas factor Xa complexes with the C-terminal truncated variant, $TFPI_{1-161}$, bind with a considerably lower affinity, which is not different from the affinity of uncomplexed factor Xa. The increased affinity of the $TFPI_{FL}$−factor Xa complex, however, appeared to be transient in the presence of an excess (over $TFPI_{FL}$) of factor Xa. This loss of affinity during the binding experiment appears to be caused by factor Xa mediated and phospholipid membrane dependent, limited proteolysis of $TFPI_{FL}$.

Our finding that the interaction of $TFPI_{FL}$ with negatively charged phospholipid membranes is extremely weak seemingly deviates from the reported binding of $TFPI_{FL}$ to acidic lipids (*13*). In that study, however, appreciable binding of $TFPI_{FL}$ alone was only observed for membranes containing 60−100% acidic phospholipid. For a lower PS content in the lipid mixture (20% PS) and in the presence of $CaCl_2$ (2.5 mM), the binding of $TFPI_{FL}$ alone was minor.

Despite its weak interaction with phospholipid membranes, $TFPI_{FL}$ in complex with factor Xa drastically enhances the phospholipid binding of factor Xa, and this enhancement apparently requires the presence of the third Kunitz domain and the C-terminus, as it is absent for the C-terminal truncated $TFPI_{1-161}$. It was suggested earlier (*13*) that the increased binding is caused by electrostatic interaction between positive charges on the C-terminus of $TFPI_{FL}$ and negative charges in the membrane. Analysis of equilibrium binding at PSPC planar bilayers (25% PS) results in an estimated value of the dissociation constant of the $TFPI_{FL}$−factor Xa complex that is about 8-fold lower, $K_d = 5$ nM, than found for factor Xa alone, $K_d = 42$ nM.

Maximal binding (Γ_{max}) of factor Xa (0.36 μg cm^{-2}) and of $TFPI_{FL}$−factor Xa complexes (0.36 μg cm^{-2}) was very similar if expressed in μg cm^{-2}, which in terms of molecules per unit area obviously implies a lower Γ_{max} for TFPI−factor Xa complexes ($\Gamma_{max} = 4.7$ pmol cm^{-2}) than for Factor Xa ($\Gamma_{max} = 8.1$ pmol cm^{-2}). This is consistent with the notion that maximal binding reflects the steric constraints of tight packing on the lipid membrane of a monolayer of protein and the reasonable assumption that the footprint on the membrane of the TFPI−factor Xa complex is increased compared to that of factor Xa. The low affinity of $TFPI_{1-161}$−factor Xa complexes entails the requirement of higher concentrations of complexes than were available to saturate the binding isotherm. This precluded the estimation of Γ_{max}. Yet, because of the similarity in maximal binding of factor Xa and $TFPI_{FL}$−factor Xa complexes, we assumed that the value of Γ_{max}, as determined for $TFPI_{FL}$−factor Xa, presents a reasonable estimation of the Γ_{max} of $TFPI_{1-161}$−factor Xa complexes.

For factor Xa and $TFPI_{1-161}$−factor Xa complexes, the K_d value estimated from the kinetics of adsorption and desorption of membrane-bound protein is in acceptable agreement to the values of the dissociation constant as estimated from equilibrium binding. For $TFPI_{FL}$−factor Xa complexes, however, we found that the desorption rate decreased with increasing time of residence at the lipid membrane. Nevertheless, when we limited the analysis to the initial phase (10 min) of desorptions initiated within 15 min after the start of the adsorption, we also found a reasonable agreement between the dissociation constants estimated from kinetics of desorption and adsorption and equilibrium binding (Table 2).

Despite this reasonable agreement between equilibrium binding and kinetics of adsorption and desorption, in all cases in which the desorption was followed for more than 20 min, deviations (see Figures 4 and 5) were observed from the model kinetics given by eq 3 with a desorption rate decreasing to a larger extent during ongoing desorption than predicted by eq 3. This indicates an increase in affinity during the desorption, a notion supported by the 3-fold decrease in desorption rate, found upon prolonged (1 h) residence at the lipid membrane. In addition, adsorption experiments in which the $TFPI_{FL}$−factor Xa containing buffer solution was repeatedly refreshed resulted in higher amounts of final adsorbed complex than found after a single addition of $TFPI_{FL}$−factor Xa complex to the buffer (data not shown), supporting again the notion of increasing affinity of $TFPI_{FL}$−factor Xa complexes with increasing residence time at the lipid membrane. Plateau levels as reached after a single addition of protein then presumably reflect a slowly decreasing solution phase concentration compensated by an equally slow increase of affinity. Presently we cannot offer an unambiguous explanation for this observation, though we speculate that the increased affinity is caused by slowly evolving intercomplex associations between tightly packed TFPI−factor complexes on the lipid membrane.

Interestingly, the high affinity binding of $TFPI_{FL}$−factor Xa complexes on PSPC membranes was found to be transient when factor Xa was present in a molar excess over TFPI. Figures 6 and 7 clearly show that the desorption of the $TFPI_{FL}$−factor Xa complex from the membrane is accompanied with limited proteolysis of $TFPI_{FL}$, yielding under reducing conditions a 26 kDa fragment and resulting in a nearly complete disappearance of the 36 kDa ($TFPI_{FL}$) band. Under the experimental conditions of Figure 6 a minor amount of the 8 kDa fragment is formed, which, however, appears considerably later than the onset of the desorption. In view of these data it is reasonable to speculate that the desorption is caused by the cleavage of the intact TFPI that results in the appearance of the 26 kDa fragment.

In separate experiments we could show that the cleavage of $TFPI_{FL}$ is dependent on the presence of both phospholipids (Figure 8) and requires a molar excess of factor Xa over TFPI. Recent work from our group (*36*) has demonstrated that the 26 kDa fragment arises from a single cleavage of $TFPI_{FL}$ at Arg^{199}−Ala^{200}, a peptide bond situated within the third Kunitz domain. The C-terminal fragment arising simultaneously, remaining invisible in Figures 7 and 8, apparently is not recognized by the anti-$TFPI_{1-161}$ antibody used in these blots.

It is interesting to bring the loss of membrane affinity attributed to the cleavage of $TFPI_{FL}$ at Arg^{199}−Ala^{200} in relation to the role to the positively charged C terminus in the TFPI−lipid interaction (*13*). It is thought that electrostatic interaction of this region of TFPI with negatively charged phospholipids mediates the enhanced affinity of the $TFPI_{FL}$−factor Xa complex, and this tallies with the observation that $TFPI_{1-161}$ in complex with factor Xa does not enhance the affinity for phospholipid membranes. The C-terminus of TFPI, however, remains covalently attached to the 26 kDa fragment via disulfide bonds upon cleavage at Arg^{199}−Ala^{200}. Therefore, we speculate that the loss of affinity is caused by a major reorientation of the TFPI C-terminus in the TFPI−factor Xa complex, resulting in a considerably increased distance between the positive charges on the C-terminus and the lipid membrane. Alternatively, dissociation of the $TFPI_{FL}$−factor Xa complex upon proteolysis could also explain a loss in binding affinity. This, however, is less likely because of the similar high affinity factor Xa binding found for $TFPI_{FL}$ and $TFPI_{1-161}$ (*11*).

The high affinity of $TFPI_{FL}$−factor Xa complexes for negatively charged membranes implies that $TFPI_{FL}$−factor Xa complexes become localized at procoagulant (negatively charged, PS-containing) membranes. Moreover, our desorption experiments show that these $TFPI_{FL}$−factor Xa complexes bound at PSPC membranes have extremely long residence times (>45 min). These long residence times were found despite experimental conditions that result in a very efficient mass transfer, with a value $\Delta = 10^{-3}$ cm s^{-1}, see eq 3.

At present it is impossible to delineate the precise functional significance of the accumulation of $TFPI_{FL}$−factor Xa complexes on procoagulant membranes. It is, however, tempting to speculate that these complexes, once located at procoagulant membranes, become extremely efficient inhibitors of the TF−factor VIIa complex. Such a mechanism could explain the difference in anticoagulant activity of full-length $TFPI_{FL}$ and C-terminal truncated $TFPI_{1-161}$. If so, then factor Xa-catalyzed cleavage of TFPI at a procoagulant membrane may present a potent regulation of the inhibition of TF−factor VIIa initiated blood coagulation.

ACKNOWLEDGMENT

We are grateful to Dr. Ole Nordfang for providing us with the recombinant C-terminal truncated TFPI variant, $TFPI_{1-161}$, and with the goat anti-human $TFPI_{1-161}$ antibody.

REFERENCES

1. Nemerson, Y. (1988) *Blood 71*, 1−8.
2. Davie, E. W., Fujikawa, K., and Kisiel, W. (1991) *Biochemistry 30*, 10363−10370.
3. Petersen, L. C., Valentin, S., and Hedner, U. (1995) *Thromb. Res. 79*, 1−47.
4. Broze, G. J., Jr., Warren, L. A., Novotny, W. F., Higuchi, D. A., Girard, J. J., and Miletich, J. P. (1988) *Blood 71*, 335−343.
5. Rapaport, S. I. (1989) *Blood 73*, 359−365.
6. Wun, T. C., Kretzmer, K. K., Girard, T. J., Miletich, J. P., and Broze, G. J., Jr. (1988) *J. Biol. Chem. 263*, 6001−6004.
7. Novotny, W. F., Girard, T. J., Miletich, J. P., and Broze, G. J., Jr. (1989) *J. Biol. Chem. 264*, 18832−18837.
8. Girard, T. J., Warren, L. A., Novotny, W. F., Likert, K. M., Brown, S. G., Miletich, J. P., and Broze, G. J., Jr. (1989) *Nature 338*, 518−520.

9. Nordfang, O., Björn, S. E., Valentin, S., Nielsen, L. S., Wildgoose, P., Beck, T. C., and Hedner, U. (1991) *Biochemistry 30*, 10371−10376.
10. Wesselschmidt, R., Likert, K., Girard, T., Wun, T. C., and Broze, G. J., Jr. (1992) *Blood 79*, 2004−2010.
11. Lindhout, T., Franssen, J., and Willems, G. (1995) *Thromb. Haemostas. 74*, 910−915.
12. Jesty, J., Wun, T. C., and Lorenz, A. (1994) *Biochemistry 33*, 12686−12694.
13. Valentin, S., and Schousboe, I. (1996) *Thromb. Haemostas. 75*, 796−800.
14. Nelsestuen, G. L., Broderius, M., and Martin, G. (1976) *J. Biol. Chem. 251*, 6886−6893.
15. Skogen, W. F., Esmon, C. T., and Cox, A. C. (1984) *J. Biol. Chem. 259*, 2306−2310.
16. Borowski, M., Furie, B. C., Goldsmith, G. H., and Furie, B. (1985) *J. Biol. Chem. 260*, 9258−9264.
17. Morita, T., and Jackson, C. M. (1986) *J. Biol. Chem. 261*, 4008−4014.
18. Nelsestuen, G. L., and Lim, T. K. (1977) *Biochemistry 16*, 4164−4171.
19. Krishnaswamy, S., Jones, K. C., and Mann, K. G. (1988) *J Biol Chem 263*, 3823−3834.
20. Cutsforth, G. A., Whitaker, R. N., Hermans, J., and Lentz, B. R. (1989) *Biochemistry 28*, 7453−7461.
21. Giesen, P. L., Willems, G. M., Hemker, H. C., and Hermens, W. T. (1991) *J. Biol. Chem. 266*, 18720−18725.
22. Cuypers, P. A., Corsel, J. W., Janssen, M. P., Kop, J. M., Hermens, W. T., and Hemker, H. C. (1983) *J. Biol. Chem. 258*, 2426−2431.
23. Corsel, J. W., Willems, G. M., Kop, J. M., Cuypers, P. A., and Hermens, W. T. (1985) *J. Colloid Interface Sci. 111*, 544−554.
24. Mertens, K., and Bertina, R. M. (1980) *Biochem. J. 185*, 647−658.
25. Lindhout, M. J., Kop-Klaassen, B. H., and Hemker, H. C. (1978) *Biochim. Biophys. Acta 533*, 327−341.
26. Smith, R. L. (1973) *J. Biol. Chem. 248*, 2418−2423.
27. Diaz-Collier, J. A., Palmier, M. O., Kretzmer, K. K., Bishop, B. F., Combs, R. G., Obukowicz, M. G., Frazier, R. B., Bild, G. S., Joy, W. D., Hill, S. R., Duffin, K. L., Gustafson, M. E., Junger, K. D., Grabner, R. W., Gallupi, G. R., and Wun, T. C. (1994) *Thromb. Haemostas. 71*, 339−346.
28. Huang, Z. F., Wun, T. C., and Broze, G. J., Jr. (1993) *J. Biol. Chem. 268*, 26950−26955.
29. Petersen, J. G., Meyn, G., Rasmussen, J. S., Petersen, J., Björn, S. E., Jonassen, I., Christiansen, L., and Nordfang, O. (1993) *J. Biol. Chem. 268*, 13344−13351.
30. Lindhout, T., Willems, G., Blezer, R., and Hemker, H. C. (1994) *Biochem. J. 297*, 131−136.
31. Brinkmann, T., Kahnert, H., Prohaska, W., Nordfang, O., and Kleesiek, K. (1994) *Eur. J. Clin. Chem. Clin. Biochem. 32*, 313−317.
32. Böttcher, C. J. F., Van Gent, C. M., and Pries, C. (1962) *Anal. Chim. Acta 24*, 203−204.
33. Giesen, P. L., Willems, G. M., and Hermens, W. T. (1991) *J. Biol. Chem. 266*, 1379−1382.
34. Andree, H. A., Hermens, W. T., and Willems, G. M. (1993) *Colloids Surf. A 78*, 133−144.
35. Spaargaren, J., Giesen, P. L., Janssen, M. P., Voorberg, J., Willems, G. M., and van Mourik, J. A. (1995) *Biochem. J. 310*, 539−545.
36. Salemink, I., Franssen, J., Willems, G. M., Hemker, H. C., and Lindhout, T. (1997) *Thromb. Haemostas. Suppl.*, 408 (abstract).

BI972194+